Assessment of inhaled cationic antibiotics in an in vitro model of Pseudomonas aeruginosa lung biofilm

Rana Awad, Sandrine Marchand, William Couet, Mohamad Nasser, Julien Buyck, Frédéric Tewes

Assessment of Inhaled Cationic Antibiotics in an *In Vitro* Model of *Pseudomonas aeruginosa* lung biofilm

Rana Awad[1], Sandrine Marchand[1,2] , William Couet[1,2], Mohamad Nasser[3], Julien M. Buyck [1], Frédéric Tewes[1*]

[1] Université de Poitiers, PHAR2, Inserm U1070, Poitiers, France.

[2] CHU de Poitiers, Laboratoire de Toxicologie et de Pharmacocinétique, Poitiers, France

[3] *PRASE, Université Libanaise, Hadath-Beirut*

* ftewes@univ-poitiers.fr

Keywords: lung infection, *Pseudomonas aeruginosa*, biofilm, *in vitro* model, tobramycin, colistin

Abstract

Objectives

This study aimed to evaluate the efficacy of inhaled cationic antibiotics, including tobramycin (TOB) and colistin (CST), using an *in vitro* alginate bead model that simulates *Pseudomonas aeruginosa* lung biofilms.

Methods

Bioluminescent *P. aeruginosa* were encapsulated within alginate beads and dispersed in either Mueller-Hinton broth (MHB) or artificial sputum medium (ASM). The impact of bead size and culture medium on TOB and CST efficacy was assessed by monitoring bioluminescence kinetics, followed by colony-forming unit (CFU/mL) measurements. Antibiotic efficacy was quantified using a Hill inhibitory model to analyze variations in CFU/mL in response to TOB and CST concentrations.

Results

The TOB EC_{50} was found to be 8-fold higher when *P. aeruginosa* was encapsulated in larger beads (1200 µm) compared to smaller beads (60 µm). TOB efficacy further decreased twofold when larger beads were dispersed in ASM. In contrast, CST demonstrated superior efficacy, being four times more potent than TOB, with corresponding EC_{50} values of 20.5 ± 2.8 times MIC and 78.4 ± 10.2 times MIC, respectively. No change in MICs was observed for either antibiotic, even after exposing bacteria to 200 times the MIC.

Conclusions

This *P. aeruginosa* biofilm model highlights how alginate and mucus modulated the efficacy of TOB and CST, and suggested the superior efficacy of CST in eradicating pulmonary biofilms.

Key words: *Pseudomonas aeruginosa*, biofilm, cationic antibiotic, pulmonary chronic infection.

1. Introduction

Pseudomonas aeruginosa (*P. aeruginosa*) is the most prevalent microorganism in the airways of adults with cystic fibrosis (CF), detected in 70% of adults aged 25 years or older [1,2]. *P. aeruginosa* pulmonary infection is a major cause of mortality in this population. *P. aeruginosa* rapidly becomes persistent and is responsible for chronic lung infections after the onset of acute infections. This persistence is notably due to its ability to colonize mucus, where it forms aggregates in a polymer matrix to create biofilms [1,3]. These biofilms are communities of various *P. aeruginosa* phenotypes, with different metabolic levels and living in an extracellular polymer matrix composed mainly of polysaccharides, extracellular DNA (eDNA) and proteins [1,3,4]. Biofilms offer protection to bacteria against host defences and antibiotics (ATBs) due to the barrier effect of the extracellular matrix and to metabolic changes in bacterial populations [3]. Therefore, new treatment strategies for bacteria present in biofilms need to be developed, and *in vitro* models mimicking biofilms formed *in vivo* are required to evaluate these strategies.

Most knowledge on *P. aeruginosa* biofilms derives from *in vitro* studies of thick (up to 1000 µm) and highly structured biofilms formed on abiotic surfaces, such as polystyrene microplates [1,2]. However, *P. aeruginosa* biofilms in the lungs of CF patients are structurally different and smaller than biofilms formed on abiotic surfaces [1]. In CF patients, *P. aeruginosa* biofilms are aggregates of 5-100 µm formed by bacteria confined in their polymeric matrix, themselves surrounded by the patients' mucus. The polymer networks that make up these two hydrogels, the lung mucus and the biofilm matrix, reduce the efficacy of cationic ATBs such as tobramycin (TOB) and colistin (CST) by limiting their diffusion to bacteria inside the biofilm [3–5]. This drop

69 in efficacy poses a clinical problem, as these two ATBs, along with levofloxacin and aztreonam,
70 are the main inhaled ATBs used to treat *P. aeruginosa* lung infections in CF patients.

71 Moreover, as chronic infection develops in these patients, new phenotypes of *P. aeruginosa*
72 appear, with high prevalence of mucoid *P. aeruginosa*, which overexpresses alginate [6–8].
73 Alginate is a polyanionic polysaccharide that gives the colony a mucoid phenotype that is typical
74 in ineradicable CF lung infection [9]. Alginate is also known to bind cationic ATBs, resulting in
75 reduction in their diffusion rate or penetration into the biofilm [10–12].

76 To take into account the specificities of pulmonary *P. aeruginosa* biofilms, several models
77 have been developed. One of the most frequently used models consists of embedding *P.*
78 *aeruginosa* into agar or alginate beads [2,13–15]. These systems mimic the basic structure of a
79 biofilm, while providing reproducible control over the composition of the system
80 [17,20,21]. Other models have attempted to mimic the unattached lung biofilm of *P. aeruginosa*
81 by growing them in a medium simulating pulmonary mucus or sputum [18–20], and suspended
82 biofilm-like structures have been described in these media. These media contain DNA and
83 mucins that can also interact with cationic ATBs [21–23], and may influence *P.*
84 *aeruginosa* biofilm development [24].

85 In the present study, the combination of alginate bead model and artificial sputum medium
86 (ASM), containing DNA and mucins, on the effects of the two major cationic ATBs, CST and TOB,
87 on *P. aeruginosa* biofilm was evaluated. The impact of several parameters, including bead size
88 and dispersion medium (ASM or cation-adjusted Muller-Hinton broth (MHB)), on the response
89 of the two ATBs was evaluated. This evaluation was based on the bioluminescence kinetics

profiles of *P. aeruginosa* and the use of a Hill-type equation to describe changes in colony-forming units as a function of ATB concentration.

2. Materials and methods

a. Materials

Experiments were performed with a bioluminescent *P. aeruginosa* strain PAO1*::luxCDABE* tagged by chromosomal integration of the *luxCDEBA* operon into the site attTn7, as described by Puja *et al.* [25]. Sodium alginate from brown algae, tobramycin base (TOB) and colistin sulfate salt (CST) were obtained from Sigma-Aldrich (Saint-Quentin-Fallavier, France). Muller-Hinton broth (MHB) and the Artificial Sputum Medium (ASM) were used for the culture of *P. aeruginosa*. ASM was composed of 5 g of mucin from pig stomach mucosa, 4 g of low molecular weight salmon sperm DNA, 1 L of sterile water, 5.9 mg of diethylene triamine penta-acetic acid (DT*PA*), 5 g of NaCl, 2.2 g of KCl, 1.81 g of Tris base, 5 g of casein hydrolysate, and 5 mL of egg yolk emulsion as described by Sriramulu Diraviam Dinesh [26]. All the compounds used in the article were purchased from Sigma-Aldrich.

b. Preparation and characterization of alginate beads loaded with *P. aeruginosa*

Fresh suspensions of the bioluminescent PAO1 strain prepared in MHB or ASM were cultured overnight at 37°C in an orbital shaker. These suspensions were washed twice with 0.9% w/v NaCl and adjusted to an OD_{600} of 0.6 (1.10^8 CFU/mL). One mL was centrifuged at 2800 g for 4 min and the pellet was dispersed in one mL of MHB or ASM. Then, *PA*O1-loaded alginate beads were prepared from 9 mL of a 2% w/v sodium alginate solution mixed with 1 mL of *PA*O1 suspension, using two different methods to produce beads depending on the desired size.

At first, small-sized beads with a diameter of about 60 µm were produced using the method proposed by Torres *et al.* [15]. Briefly, the alginate-bacteria mix was emulsified for 5 minutes at 600 rpm in 150 mL of paraffin oil supplemented by 0.01% w/v of sorbitan monostearate nonionic surfactant using a blade stirrer (Heidolph mechanical agitators, RZR 2021, Germany).

Then, 20 mL of 0.1 M TRIS-HCl buffer pH 7 containing 0.1 M $CaCl_2$ was added dropwise to the emulsion and kept under stirring for 90 min to harden the beads. The beads were then centrifuged at 2800 g for 10 min and washed several times with 0.9% m/v of NaCl. The mCherry fluorescent PA01-loaded beads were characterized by confocal laser scanning microscopy (CLSM). Visualization was performed on an Olympus FluoView FV-3000 equipped with an IX83 confocal laser scanning microscope (40x magnification). To study the fluorescence of the mCherry protein produced by PA01, samples were excited at 561 nm and emission was observed between 570 and 670 nm. For each condition, 40 to 50 stacks of horizontal plane images (1024×1024 pixels corresponding to 200×200 µm) with a z-step of 0.5 µm were acquired. Three-dimensional projections of the beads' interior were constructed using the Easy 3D function of the IMARIS software (Bitplane). Consistent segmentation parameters (particle size, absolute intensity, and absence of post-segmentation filters) were applied to all 3D constructs.

A second method previously described by Bjarnsholt *et al.* [27] was used to produce larger beads, with a diameter of around 1200 µm. The alginate-bacteria mixture was poured into a 1 mL repeating pipette (Eppendorf Multipette® plus, France), the tip of which was placed 1 cm above the surface of a sterile $CaCl_2$ Tris-HCl buffer solution (0.05 M, pH=7) with stirring. Droplets of 2 µL of the mixture were released to produce beads that were cured for one hour in Tris-HCl, $CaCl_2$. The beads were then washed with 0.9% NaCl. Their diameter was estimated with a microscope (Macroview olympus MVX10, France) by measuring between 50 to 100 beads.

c. Time-luminescence kinetics

To characterize the dynamics of the antimicrobial effects of CST and TOB against *P. aeruginosa* loaded in alginate beads, bioluminescence kinetics were measured in the presence

of different concentrations of ATB in the culture media (MHB or ASM). Twenty-four-hour-old alginate beads were dispersed in the growth medium to obtain a bioluminescence value of 20,000 ± 10,000 RLU (Relative Light Unit), measured by a plate reader, allowing an increase or decrease in signal to be observed (Tecan, Austria Gmbh, Infinite 200® PRO). After which, 100 µL of bead suspension was dispensed into non-binding (to avoid adherent biofilm formation), white, 96-well microplates (Greiner bio-one, France), followed by 100 µL of concentrated ATB solution in MHB or ASM, leading to final concentrations of 0.25, 0.5, 1, 2, 5, 10, 25, 50, 100 and 200 times the MIC of each ATB. The MICs of TOB and CST against PAO1, determined as described in paragraph "f", were equal to 0.5 mg/L and 1 mg/L, respectively. The plates were sealed with a clear, gas-permeable, moisture barrier membrane, and luminescence was monitored every 30 min for 40 h using the plate reader Infinite® 200 PRO. Controls without ATB were utilized to assess the effect of the medium on bacterial growth. Controls without bacteria were used to verify the absence of contamination.

d. Viable cell counts after time-luminescence kinetics.

After 40 h of exposure to the ATB, the *P. aeruginosa* trapped in the beads were released by solubilizing the alginate as recommended by Bjarnsholt *et al.* [27]. Wells were washed with an aqueous solution containing 0.05 M of $NaHCO_3$ and 0.02 M of citric acid and the final volume was adjusted to 1 mL. After shaking for 30 min, the solutions were serially diluted in 0.9% m/v NaCl and plated on MH agar. The plates were incubated at 37°C and numbers of CFU were counted after 24, 48 and 72 h. The total number of CFUs was used for data analysis and modelling.

e. Data analysis and modelling

RStudio software version "1.2.1335" and the "ggplot2 version 3.10" package were used to plot the smoothed average luminescence values against time using a Generalized Additive Model (GAM) as the smoothing method. The shaded area around the mean value curve is the 95% confidence level interval for the mean values predicted by the GAM smoothing model.

The antibacterial effect of TOB and CST obtained under the different conditions tested (effect of bead size and dispersion medium) was studied by modelling the CFU/mL counted after 40 hours of exposure to the ATBs as a function of their concentrations (*C*) expressed as multiples of MIC. The modeling was done using an inhibitory Hill equation (Equation 1):

$$CFU = CFU_0 - \frac{(CFU_0 - CFU_\infty) \times C^\gamma}{EC_{50}^\gamma + C^\gamma} \qquad \text{(Equation 1)}$$

In Equation 1, CFU_0 refers to the mean CFU/mL measured in the absence of ATB. CFU_∞ refers to the lowest mean CFU/mL value when the ATB concentration tends to infinity. EC_{50} is the ATB concentration needed to achieve 50% of CFU_0 and γ is the slope factor (Hill coefficient) that measures the susceptibility of *P. aeruginosa* survival within the ATB concentration range. The predicted mean CFU/mL was evaluated for each ATB concentration based on the hypothesis that individual CFU/mL values were normally distributed around the mean value with a standard deviation. Parameters were evaluated using Rstan version 2.19.3, run under RStudio software, by performing Bayesian analysis of the data and using the following weakly informative prior distributions: the log of CFU_0 is uniformly distributed between 5 and 10, EC_{50} is normally distributed between 0 and 100, and γ between 0 and 10. Simulations were run for six chains

with 1000 burn-in steps followed by 1000 Markov chain Monte Carlo (MCMC) steps. CFU/mL values below the limit of quantification (25 CFU/mL) were set at 1 CFU/mL for analysis.

f. Change in MIC after exposure to antibiotics.

To determine whether bacteria surviving exposure to high concentrations of ATB is the result of the development of a resistance mechanism, MIC measurements were made from colonies collected on agar plates that grew after 40 hours of ATB exposure. Colonies were suspended in MHB and the OD_{600} was adjusted to 0.6. The suspension was then diluted 100-fold in MHB to obtain 1.10^6 CFU/mL and 100 µL were distributed to the wells of a 96-well plate. Then, 100 µL of 2-fold concentrated ATB solution was added to obtain final concentrations of 0.125, 0.25, 0.5, 1, 2, 4, 8, 16, 32, and 64 mg/L and 5.10^5 CFU/mL of *P. aeruginosa*. The plates were incubated at 37 °C in an orbital shaker (150 rpm, Advantage Lab, ALOS - 0.5) and OD_{600} was read after 18 h – 20 h using the Infinite® 200 PRO plate reader (Tecan, France).

3. Results

a. Characterization of *P. aeruginosa*-loaded alginate beads

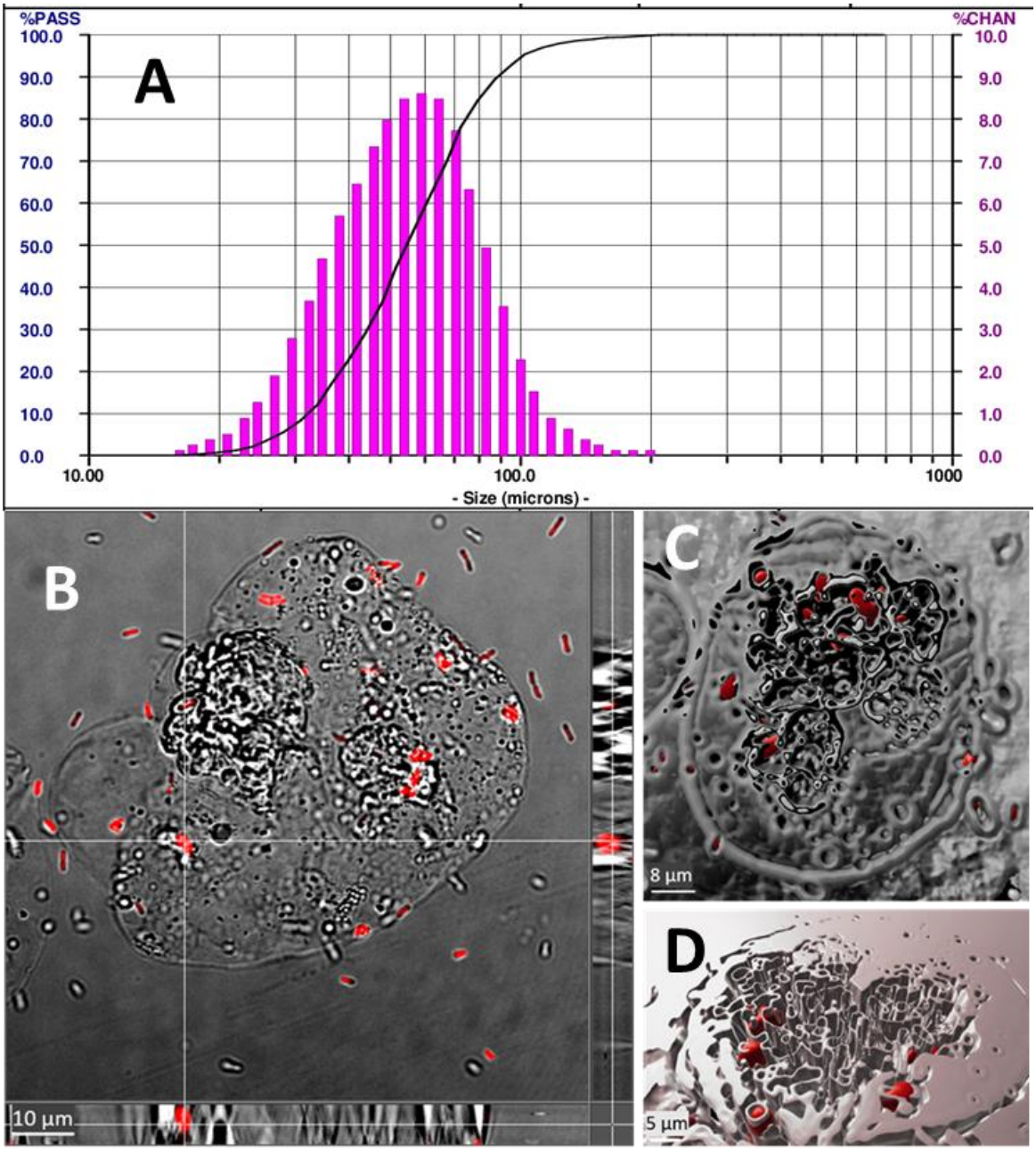

Figure 1: Characterization of Small Alginate Beads. A) Bead size distribution as determined by laser diffraction. B) Confocal laser scanning microscopy micrograph of beads loaded with mCherry-expressing PAO1. C-D) Three-dimensional projections illustrating the internal structure of the beads.

Small beads were prepared by emulsifying a 2% alginate solution in paraffin oil, followed by gelation with the addition of a Ca^{2+} solution. The particle size distribution was characterized, showing a monodisperse profile with a median diameter of 60 µm (Fig. 1A). Bead structure and the distribution of PAO1 within the beads were visualized using confocal laser scanning microscopy (CLSM) with mCherry-expressing PAO1-loaded beads. The results showed that small PAO1 aggregates, each less than 10 µm in size, were dispersed within the structured, channeled beads, allowing fluid access throughout the beads (Fig. 1 B-D). *P. aeruginosa* was observed both as micro-aggregates within the beads and as planktonic cells capable of escaping from the beads.

b. Effect of bead size on tobramycin efficacy

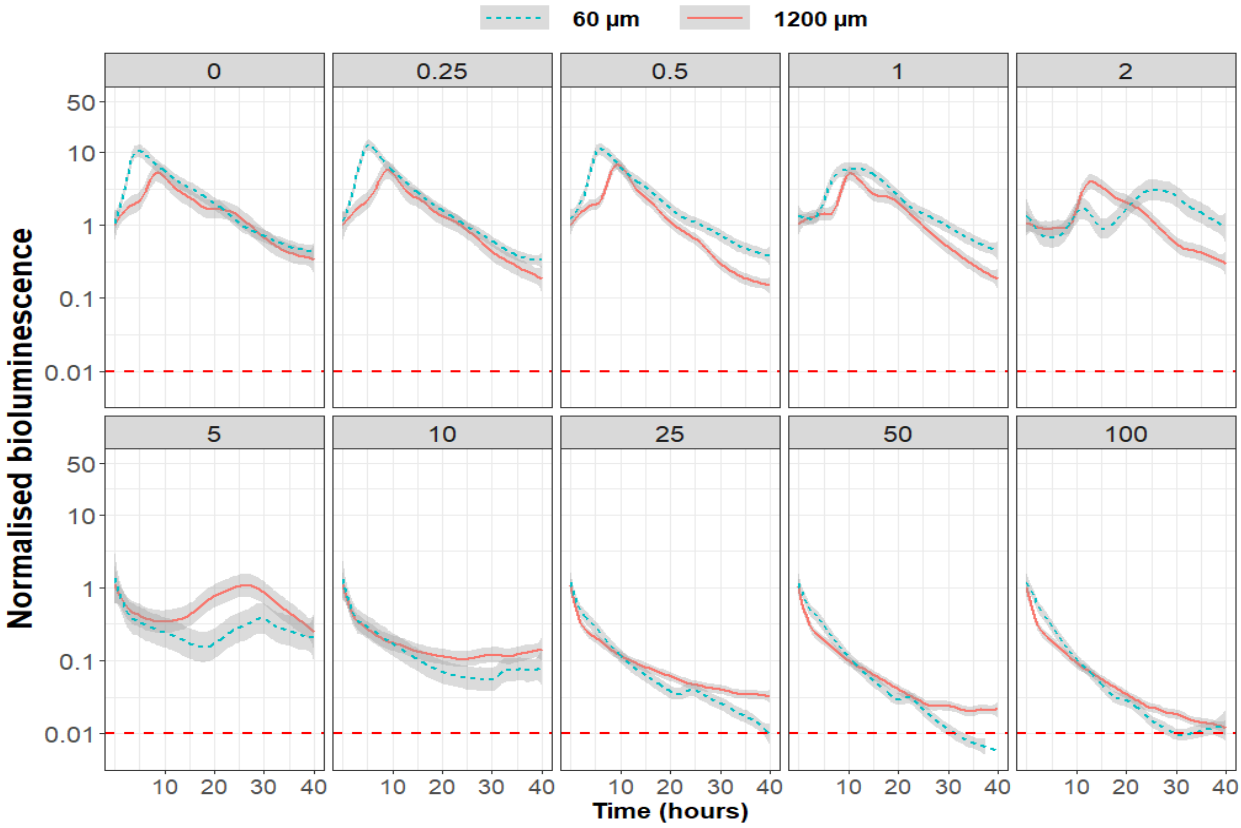

Figure 2. Bioluminescence kinetics of *P. aeruginosa* trapped in 60 or 1200 µm diameter alginate beads dispersed in MHB containing different concentrations of TOB (expressed in

number of times the MIC). For each well, the luminescence intensity was normalized to the value measured at time zero. The gray band around the curves is the 95% confidence level interval of the mean values predicted by the GAM smoothing model from 12 to 16 experiments (n = 12-16). The red horizontal dashed line is the limit of accuracy of the plate reader.

The first parameter investigated was effect of bead size on antibiotic efficacy. Luminescence kinetics of *P. aeruginosa* trapped in alginate beads of 60 and 1200 µm of average diameter dispersed in MHB containing various concentrations of TOB were recorded for 40 hours (Fig. 2). In the absence of TOB, the luminescence profiles obtained with both bead sizes initially showed an increase in signal to a maximum level, followed by a zero-order decrease for the rest of the time. The initial increase in luminescence was slower with large beads than with small beads, resulting in a 5-hour time lapse in reaching maximum luminescence (Fig. 2, first upper panel). Addition of TOB at a concentration below the MIC (MIC_{TOB}= 0.5 mg/L) had no effect on the luminescence kinetics with either type of bead. At TOB concentrations above the MIC and up to 25 MIC, the initial increase in luminescence was replaced by a decline, of which the intensity increased progressively with TOB concentration. For TOB concentrations of 2 to 10 times the MIC, this decrease was more intense with small beads (60 µm) than with large ones (1200 µm). To further analyze the effect of bead size on TOB efficacy, the CFU/mL of *P. aeruginosa* present at the end of the 40-hour kinetics was measured (Figure 3 A and B).

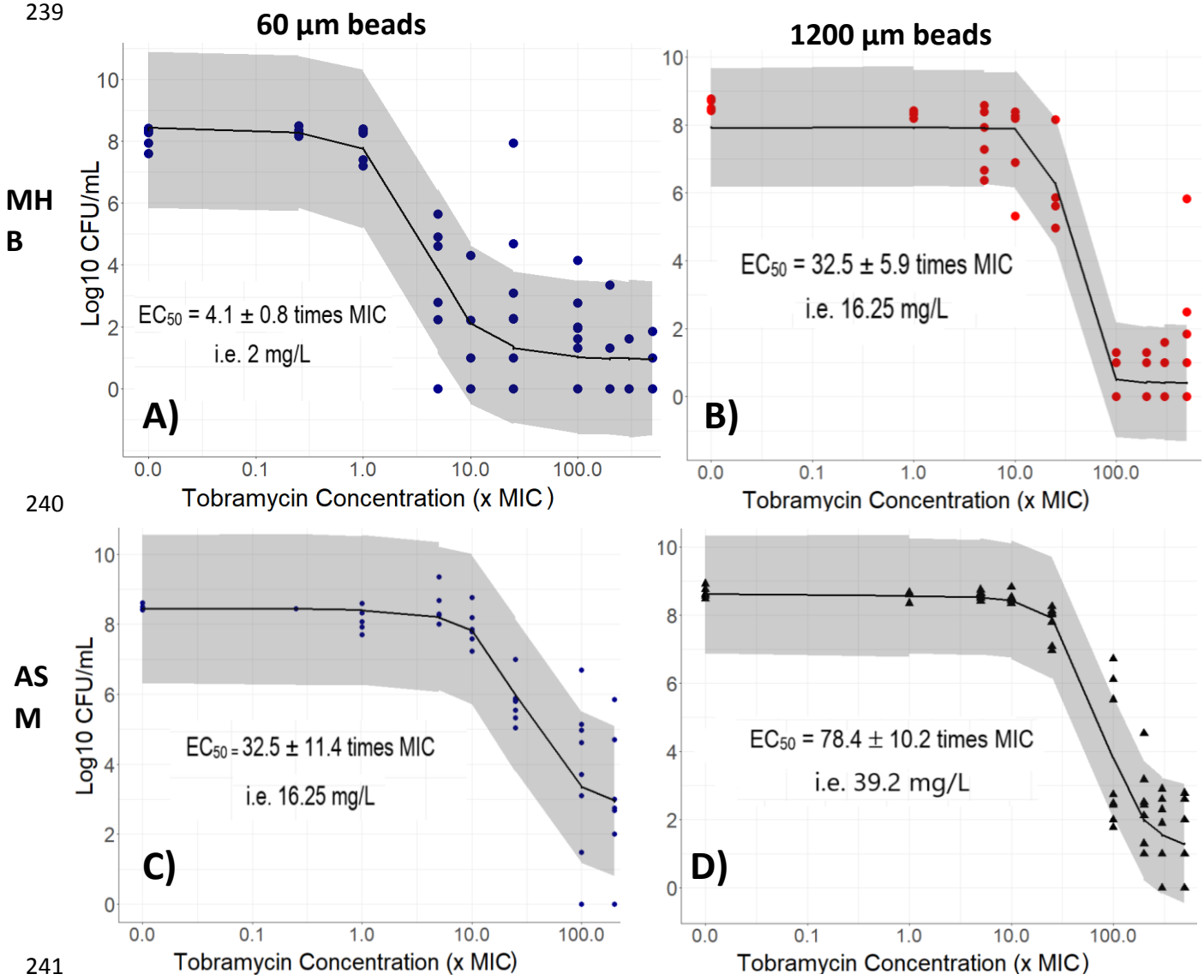

Figure 3. Log10 CFU/mL of *P. aeruginosa* in function of TOB concentration measured after 40 h of exposure for A) *P. aeruginosa* trapped in 60 µm diameter beads dispersed in MHB, B) *P. aeruginosa* trapped in 1200 µm diameter beads dispersed in MHB, C) *P. aeruginosa* trapped in 60 µm beads dispersed in ASM, and D) *P. aeruginosa* trapped in 1200 µm beads dispersed in ASM. The shaded areas are the 95% credible intervals around the predicted mean values (lines) obtained using the Hill equation (Eq. 1). All points below the limit of quantification (25 CFU/mL) were set to 1 CFU/mL.

The number of CFU/mL present in the alginate beads after 40 hours of contact with various concentrations of TOB in MHB is presented in Fig. 3A for 60 µm beads and 2B for 1200 µm beads. For both bead sizes, the profiles showing log CFU/mL of *P. aeruginosa* versus TOB concentration in MHB exhibited a sigmoidal shape described by the Hill equation (Eq.1), with over 95% of the experimental points falling within the 95% credibility interval around the predicted mean values. Indeed, the mean values predicted by the model are centered between the individual points, and the 95% credible intervals represented by a grey area in Fig. 3 encompass approximately 95% of the individual values. However, a steeper slope of the sigmoid curve was obtained for 1200 µm beads, showing a significant change in *P. aeruginosa* CFU/mL for TOB concentrations between 25 and 50 times the MIC (Fig. 3B). In addition, the EC_{50} value calculated for the 60 µm beads (4.1 ± 0.8 times MIC) was 8-fold lower than for the 1200 µm beads (32.5 ± 5.9 times MIC). Bacteria were still present in both types of bead in the presence of 200 times the MIC in TOB (data not shown), but no change in MIC against this antibiotic, measured on colonies collected on plates used for CFU counting, was observed after exposure to these concentrations.

c. Effect of culture medium on tobramycin efficacy.

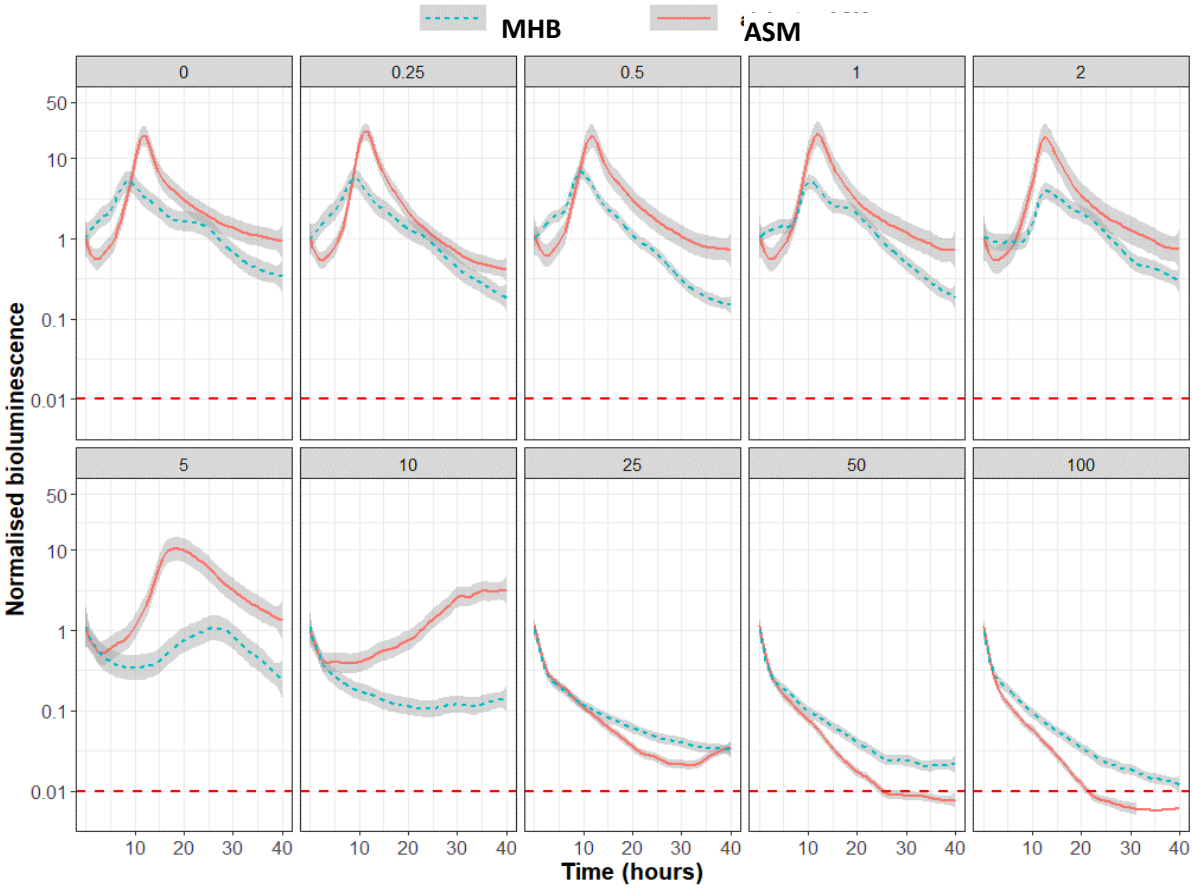

Figure 4. Bioluminescence kinetics of *P. aeruginosa* trapped in beads of 1200 µm diameter dispersed in MHB or ASM containing various concentrations of TOB (expressed in number of times TOB MIC (0.5 mg/L)). For each well, luminescence intensity was normalized to the value measured at time zero. The gray band around the lines is the 95% confidence level interval of the mean values predicted from the GAM smoothing model from 12 to 16 experiments. The red dashed line is the limit of accuracy of the plate reader.

The second parameter evaluated was the composition of the medium dispersing the alginate beads, replacing conventional MHB with a medium simulating the composition of lung mucus (ASM). Bioluminescence kinetics obtained with large beads dispersed in MHB or ASM containing different concentrations of TOB are shown in Fig. 4 for large beads and in Fig. S1 for smaller beads. TOB had virtually no effect on the luminescence profiles obtained in ASM for concentrations up to 2 times the MIC. For TOB concentrations between 5 and 10 MICs, the

luminescence measured in ASM was significantly higher than in MHB. Above 25 MICs, the luminescence recorded in ASM was less than or equal to that recorded in MHB. The effect of changing the medium on the luminescence kinetics recorded for small beads was similar to that observed for large beads (Figure S1: supplementary materials).

The evolution of the concentration of *P. aeruginosa* capable of multiplying after 40 h of treatment as a function of the concentration of TOB in ASM is shown in Fig. 3C and Fig. 3D for small and large beads, respectively. In this medium, TOB was less efficient than in MHB, as indicated by the increase in EC_{50} values. For the small beads, EC_{50} increased 8 times between MHB (4.1 ± 0.8 times MIC) and ASM (32.5 ± 11.4 times MIC). It more than doubled in ASM (78.4 ± 10.2 times MIC) compared to MHB (32.5 ± 5.9 times MIC) for large beads. EC_{50} was only doubled in ASM when the bead size increased from 60 to 1200 µm, while an 8-fold increase in the EC_{50} was observed in MHB for the same change in bead size (Fig. 3). Again, while the bacteria in the beads survived a TOB concentration 200 times the MIC, no change in MIC was observed for these bacteria.

d. Comparison between tobramycin and colistin efficacy

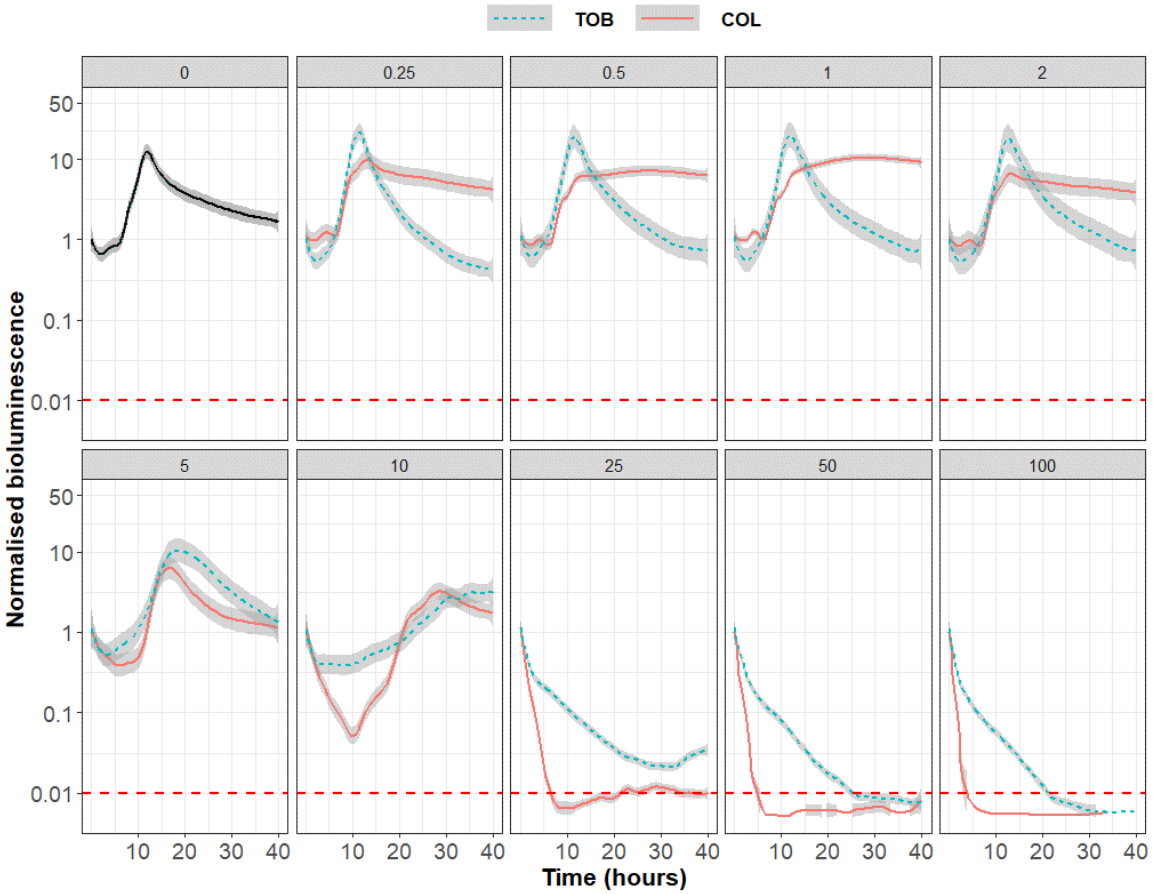

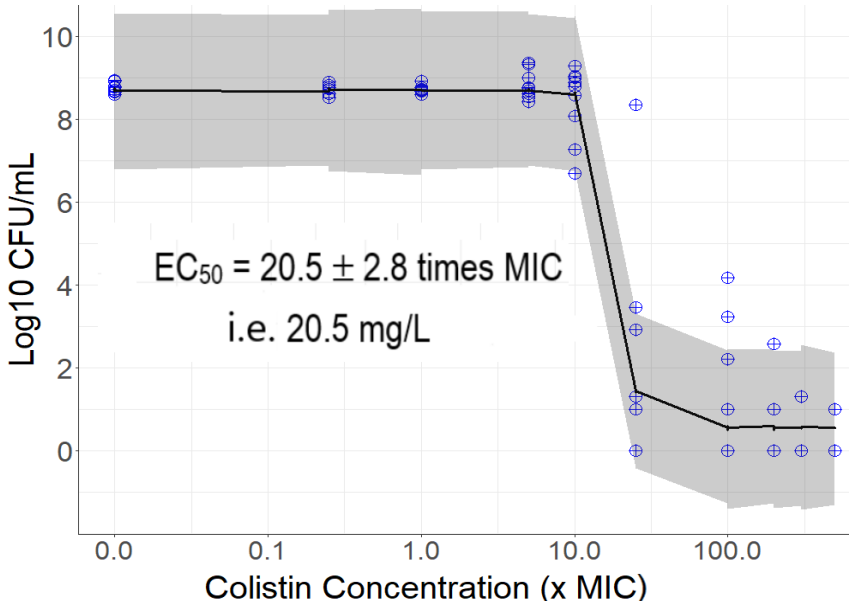

Figure 5. Upper panels: Bioluminescence kinetics of *P. aeruginosa* trapped in large alginate beads dispersed in ASM exposed to various CST or TOB concentrations (MIC_{TOB} = 0.5 mg/L, MIC_{COL} = 1 mg/L). For each well, luminescence intensity was normalized to the value measured at time zero. The gray band around the lines is the 95% confidence level interval of the mean

values predicted from the GAM smoothing model (n = 12-16). The red dashed line is the limit of accuracy of the plate reader. Lower panel: Total bacterial concentration (Log10 CFU / mL) obtained after 40 h of exposure of *P. aeruginosa* trapped in 1200 µm diameter beads to various concentrations of CST. The shaded areas are the 95% credible intervals around the predicted mean values (lines) obtained using the Hill model (Eq. 1).

To assess the effect of another type of cationic ATB, the efficacy of CST was evaluated using the large beads dispersed in ASM, i.e. under conditions where TOB was less effective. While TOB had no effect on luminescence profiles obtained at concentrations up to two times the MIC, CST induced the formation of a plateau after reaching maximum luminescence for concentrations ranging from 0.25 to two times the MIC (Fig. 5). At five times the MIC, CST and TOB had the same effect on luminescence profiles. From 10 times the MIC, CST induced a quick decrease in luminescence over 10 hours that was followed by a restart in light production. Above 25 times the MIC, luminescence decreased even more rapidly and intensely with CST to reach the limit of accuracy of the plate reader in less than 10 hours. In comparison, the luminescence produced by *P. aeruginosa* in contact with TOB decreased half as rapidly as with CST, reaching the plate reader's accuracy limit only after 20 hours.

The profile of the concentration of surviving *P. aeruginosa* relative to the concentration of CST is shown in the lower panel of Fig. 5. The data obtained with CST were also fitted with the Hill model (Eq. 1). The EC_{50} value obtained with CST was four times lower than that observed with TOB (20.5 $\pm$ 2.8 times MIC for CST vs 78.4 $\pm$ 10.2 times MIC for TOB, respectively). In addition, a steeper slope of the sigmoid curve was obtained with CST than with TOB, showing an "all or nothing" type effect of CST. Thus, a slight increase in the concentration of CST above the EC_{50} eliminates almost all bacteria.

4. Discussion

In this study, alginate bead-based models of *P. aeruginosa* biofilms were used to assess the efficacy of two cationic ATBs conventionally administered as aerosols to treat chronic *P. aeruginosa* infections in CF patients. In CF lungs, *P. aeruginosa* biofilms are small bacterial aggregates, typically ranging from 5 to 50 µm in size [1]. We designed the experimental conditions to mirror these clinical observations by using a short biofilm development period (24 hours), which produced aggregates approximately 10 µm in diameter, as measured by confocal laser scanning microscopy (CLSM). These dimensions are consistent with bacterial clusters observed both in CF patients and in prior alginate bead models [13].

a. Characterization of bioluminescent *Pseudomonas*-loaded alginate beads

Most studies assess ATB efficacy at a single endpoint, often through techniques like crystal violet staining or metabolic activity assays. Such methods, however, do not account for the dynamic evolution of biofilms under antibiotic pressure. In contrast, the bioluminescence-based kinetics used here allowed us to monitor bacterial viability and metabolic activity continuously. This latter parameter depends on the availability of bacterial enzymes (luciferase, ATP synthase, etc.) and substrates (O_2, sugars, etc.) in the culture medium [34,35]. The bioluminescence profiles observed in the absence of ATB (Fig. 2, panel "0"; Fig. 4, panel "0") resembled typical bacterial growth curves expressed in CFU/mL, with an exponential phase followed by a gradual decline, although a stationary phase was absent. This absence may indicate a stable bacterial count with reduced metabolic activity due to nutrient depletion, resulting in diminished light production, as previously reported [35].

In the absence of ATB, increasing the bead size delayed the peak of bioluminescence in the kinetics. Smaller beads (60 µm) offer a higher surface area-to-volume ratio, promoting better diffusion of oxygen and nutrients, which facilitates bacterial growth and activity. Larger beads (1200 µm), by contrast, hinder diffusion, leading to slower bacterial growth while still reaching a comparable final bacterial load of approximately 5 x 10^8 CFU/mL after 40 hours of incubation (Fig. 3 and 5).

b. Modulating tobramycin efficacy through bead size and culture medium composition.

In the CF patients' lungs, *P. aeruginosa* aggregates are confined in an alginate-based matrix and dispersed in the thick mucus of the patients. Both alginate-based matrix and mucus create barriers that can limit the diffusion of ATBs with stronger effect on cationic ones [4,11,28–31]. In CF patients, TOB is often used as an aerosol treatment during the early stages of lung infection, before chronic biofilm formation [32,33]. Thus, biofilm development frequently occurs under TOB selection pressure, a factor we replicated in this *in vitro* model.

To test the influence of certain parameters of the *P. aeruginosa* lung biofilm model, the size of the alginate beads mimicking the biofilm matrix and the nature of the dispersion medium representing mucus were changed to assess their effect on the efficacy of TOB. While prior studies have explored these factors independently [13,16,29], our study is the first to manipulate them simultaneously to assess their combined impact on TOB effectiveness. Both increasing bead size from 60 to 1200 µm and replacing MHB with a mucus-like culture medium increased TOB's EC_{50} by a factor of 8, suggesting reduced antibiotic efficacy. When both conditions were altered, the EC_{50} increased 16-fold, indicating an additive effect. These results are in agreement with previous studies, which showed that alginate and mucus component

368 reduce TOB efficacy. Indeed, Cao *et al* [29] showed on an alginate bead biofilm model that the
369 binding of TOB to a multitude of sites led to a pronounced delay in its diffusion into the biofilm.
370 This slowing of the increase in free TOB concentration inside the beads could increase the
371 probability of adaptation and survival of bacteria residing in biofilms [34,35]. Likewise, *P.*
372 *aeruginosa* biofilms grown on glass surface coated with mucins, the glycoproteins present in
373 mucus, establish large aggregates, and increase tolerance to TOB compared to biofilms grown
374 on glass coated with actin or DNA [24]. Several considerations may explain the reduced efficacy
375 of TOB in the presence of mucus components. For example, several studies have shown that
376 mucins can bind to TOB, reducing its immediate availability and diffusion through mucus [4,11].
377 Some studies also suggest that mucins have an effect on bacterial phenotype and promote
378 biofilm formation as well as reducing ATB diffusion [4,11,24]. In addition, it has been shown
379 that the lipid composition in media mimicking CF mucus can influence the lipid composition of
380 *P. aeruginosa* membranes, reducing their permeability to certain ATBs [36]. Extracellular DNA in
381 mucus can also bind to TOB, further impeding its efficacy [22].

382 **c. Superior efficacy of colistin versus tobramycin in the lung biofilm model.**

383 All the parameters evaluated in this study showed that CST was more effective than TOB in
384 controlling the concentration of *P. aeruginosa* in the lung biofilm model, particularly in larger
385 beads dispersed in ASM. Indeed, in bioluminescence kinetics, the two ATBs had the same effect
386 for concentrations up to 5 times their MIC, but from 25 MIC, CST was able to rapidly reduce the
387 bioluminescence below the precision limit of the plate reader, while the effect of TOB was
388 slower and less intense. In colony counts, CST was 4 times more effective than TOB relatively to
389 their own MIC, as indicated by their respective EC_{50} values of 20.5 ± 2.8 times the MIC (Fig. 5)

and 78.4 ± 10.2 times the MIC (Fig. 3D). In addition, the effect of TOB was gradual around its EC_{50} value, while the effect of CST was closer to an "all or nothing" effect, as shown by the steeper slope obtained with CST on the graph showing the variation of log CFU versus log ATB concentration in Fig. 5. Indeed, the slope factor or Hill coefficient parameter that was used to describe the evolution of the *P. aeruginosa* concentration in function of ATBs concentration was very high for CST (>10), suggesting high susceptibility of *P. aeruginosa* to CST once its appropriate concentration (EC_{50}) is reached, similar to stop and go behavior.

Hence, easier control of the bacterial population is expected with CST once its concentration slightly exceeds the EC_{50} value, with less chance of selecting resistant bacteria. A few previously published studies have compared the effect of CST and TOB on *P. aeruginosa* in the presence of mucus and the results may seem discordant. Some are in accordance with our results and show that CST effect was less impacted than TOB effect by the presence of mucins and alginate. Indeed, Muller *et al.* [4] found a significant reduction of TOB efficacy on *P. aeruginosa* biofilms grown in the presence of mucus compared with those grown in its absence while the influence of human mucus on CST efficacy was almost negligible. On the contrary, several studies have shown that components of mucus or sputum such as mucins reduce the effectiveness of CST and other polymyxins against *P. aeruginosa*, mainly due to their ability to bind to them [26,28,39–41].

Interestingly, bioluminescence kinetics measured at CST concentrations below 5 MIC showed stable light production once the maximum value was reached, instead of the slow decrease observed in the absence of ATB or with TOB. This result suggests that low concentrations of CST stimulate bacterial metabolic activity. In this sense, previous studies have

suggested that colistin stimulates the tricarboxylic acid (TCA) cycle, which in turn leads to increased NADH production and enhanced respiration rates. [37,38]. This metabolic stimulation could explain the observed stability in light production at sub-inhibitory CST concentrations.

5. Conclusion

This study shows that *Pseudomonas aeruginosa* trapped in alginate, as occurs in the lung biofilms of CF patients, can persist even when exposed to high concentrations of TOB or CST without developing resistance to these antibiotics. This decrease in efficacy poses a clinical problem, as these two antibiotics are the main ATBs used by inhalation to treat *Pseudomonas aeruginosa* lung infections in these patients. The sensitivity of *Pseudomonas aeruginosa* incorporated in alginate beads can be adjusted by modifying bead size and dispersion medium, demonstrating the influence of alginate and mucus on the efficacy of these antibiotics. Bioluminescence measurements and colony counts show that CST is more effective than TOB on this *in vitro* model of *Pseudomonas aeruginosa* lung biofilms.

6. References

1. Bjarnsholt, T.; Alhede, M.; Alhede, M.; Eickhardt-Sørensen, S.R.; Moser, C.; Kühl, M.; Jensen, P.Ø.; Høiby, N. The in Vivo Biofilm. *Trends Microbiol.* **2013**, *21*, 466–474, doi:http://dx.doi.org/10.1016/j.tim.2013.06.002.

2. Coenye, T.; Nelis, H.J. In Vitro and in Vivo Model Systems to Study Microbial Biofilm Formation. *J. Microbiol. Methods* **2010**, *83*, 89–105, doi:10.1016/j.mimet.2010.08.018.

3. Bahamondez-Canas, T.F.; Zhang, H.; Tewes, F.; Leal, J.; Smyth, H.D.C. PEGylation of Tobramycin Improves Mucus Penetration and Antimicrobial Activity against *Pseudomonas aeruginosa* Biofilms in Vitro. *Mol. Pharm.* **2018**, *15*, 1643–1652, doi:10.1021/acs.molpharmaceut.8b00011.

4. Braun, A.; Sewald, K.; Müller, L.; Wronski, S.; Murgia, X.; Lehr, C.-M.; Börger, C.; Siebenbürger, L.; Hittinger, M.; Schwarzkopf, K.; et al. Human Airway Mucus Alters Susceptibility of *Pseudomonas aeruginosa* Biofilms to Tobramycin, but Not Colistin. *J. Antimicrob. Chemother.* **2018**, *73*, 2762–2769, doi:10.1093/jac/dky241.

5. Mucus and Mucin Environments Reduce the Efficacy of Polymyxin and Fluoroquinolone Antibiotics against *Pseudomonas aeruginosa* | ACS Biomaterials Science & Engineering Available online: https://pubs-acs-org.proxy.insermbiblio.inist.fr/doi/pdf/10.1021/acsbiomaterials.8b01054 (accessed on 16 October 2020).

6. Maunders, E.; Welch, M. Matrix Exopolysaccharides; the Sticky Side of Biofilm Formation. *FEMS Microbiol. Lett.* **2017**, *364*, doi:10.1093/femsle/fnx120.

7. Sousa, A.; Pereira, M. *Pseudomonas aeruginosa* Diversification during Infection Development in Cystic Fibrosis Lungs—A Review. *Pathogens* **2014**, *3*, 680–703, doi:10.3390/pathogens3030680.

8. Leid, J.G.; Willson, C.J.; Shirtliff, M.E.; Hassett, D.J.; Parsek, M.R.; Jeffers, A.K. The Exopolysaccharide Alginate Protects *Pseudomonas aeruginosa* Biofilm Bacteria from IFN-γ-Mediated Macrophage Killing. *J. Immunol.* **2005**, *175*, 7512–7518.

9. Hassett, D.J.; Sutton, M.D.; Schurr, M.J.; Herr, A.B.; Caldwell, C.C.; Matu, J.O. *Pseudomonas aeruginosa* Hypoxic or Anaerobic Biofilm Infections within Cystic Fibrosis Airways. *Trends Microbiol.* **2009**, *17*, 130–138, doi:10.1016/j.tim.2008.12.003.

10. Nichols, W.W.; Dorrington, S.M.; Slack, M.P.; Walmsley, H.L. Inhibition of Tobramycin Diffusion by Binding to Alginate. *Antimicrob. Agents Chemother.* **1988**, *32*, 518–523, doi:10.1128/AAC.32.4.518.

11. Tseng, B.S.; Zhang, W.; Harrison, J.J.; Quach, T.P.; Song, J.L.; Penterman, J.; Singh, P.K.; Chopp, D.L.; Packman, A.I.; Parsek, M.R. The Extracellular Matrix Protects *Pseudomonas aeruginosa* Biofilms by Limiting the Penetration of Tobramycin: Limited Tobramycin Penetration Protects Biofilms. *Environ. Microbiol.* **2013**, n/a-n/a, doi:10.1111/1462-2920.12155.

12. Walters, M.C.; Roe, F.; Bugnicourt, A.; Franklin, M.J.; Stewart, P.S. Contributions of Antibiotic Penetration, Oxygen Limitation, and Low Metabolic Activity to Tolerance of *Pseudomonas aeruginosa* Biofilms to Ciprofloxacin and Tobramycin. *Antimicrob. Agents Chemother.* **2003**, *47*, 317–323, doi:10.1128/AAC.47.1.317-323.2003.

13. Sønderholm, M.; Kragh, K.N.; Koren, K.; Jakobsen, T.H.; Darch, S.E.; Alhede, M.; Jensen, P.Ø.; Whiteley, M.; Kühl, M.; Bjarnsholt, T. *Pseudomonas aeruginosa* Aggregate Formation in an Alginate Bead Model System Exhibits In Vivo-Like Characteristics. *Appl. Environ. Microbiol.* **2017**, *83*, doi:10.1128/AEM.00113-17.

14. Pedersen, S.S.; Shand, G.H.; Hansen, B.L.; Hansen, G.N. Induction of Experimental Chronic *Pseudomonas aeruginosa* Lung Infection with *P. Aeruginosa* Entrapped in Alginate Microspheres. *APMIS* **1990**, *98*, 203–211, doi:10.1111/j.1699-0463.1990.tb01023.x.

15. Torres, B.G.S.; Awad, R.; Marchand, S.; Couet, W.; Tewes, F. In Vitro Evaluation of *Pseudomonas aeruginosa* Chronic Lung Infection Models: Are Agar and Calcium-Alginate Beads Interchangeable? *Eur. J. Pharm. Biopharm.* **2019**, *143*, 35–43, doi:10.1016/j.ejpb.2019.08.006.

16. Xu, X.; Stewart, P.S.; Chen, X. Transport Limitation of Chlorine Disinfection of *Pseudomonas aeruginosa* Entrapped in Alginate Beads. *Biotechnol. Bioeng.* **1996**, *49*, 93–100, doi:10.1002/(SICI)1097-0290(19960105)49:1<93::AID-BIT12>3.0.CO;2-C.

17. Sønderholm, M.; Koren, K.; Wangpraseurt, D.; Jensen, P.Ø.; Kolpen, M.; Kragh, K.N.; Bjarnsholt, T.; Kühl, M. Tools for Studying Growth Patterns and Chemical Dynamics of Aggregated *Pseudomonas aeruginosa* Exposed to Different Electron Acceptors in an Alginate Bead Model. *Npj Biofilms Microbiomes* **2018**, *4*, 3, doi:10.1038/s41522-018-0047-4.

18. Sriramulu, D.D.; Lünsdorf, H.; Lam, J.S.; Römling, U. Microcolony Formation: A Novel Biofilm Model of *Pseudomonas aeruginosa* for the Cystic Fibrosis Lung. *J. Med. Microbiol.* **2005**, *54*, 667–676, doi:10.1099/jmm.0.45969-0.

19. Haley, C.L.; Colmer-Hamood, J.A.; Hamood, A.N. Characterization of Biofilm-like Structures Formed by *Pseudomonas aeruginosa* in a Synthetic Mucus Medium. *BMC Microbiol.* **2012**, *12*, 181, doi:10.1186/1471-2180-12-181.

20. Pritchard, M.F.; Powell, L.C.; Jack, A.A.; Powell, K.; Beck, K.; Florance, H.; Forton, J.; Rye, P.D.; Dessen, A.; Hill, K.E.; et al. A Low-Molecular-Weight Alginate Oligosaccharide Disrupts Pseudomonal Microcolony Formation and Enhances Antibiotic Effectiveness. *Antimicrob. Agents Chemother.* **2017**, *61*, doi:10.1128/AAC.00762-17.

21. Okshevsky, M.; Meyer, R.L. The Role of Extracellular DNA in the Establishment, Maintenance and Perpetuation of Bacterial Biofilms. *Crit. Rev. Microbiol.* **2015**, *41*, 341–352, doi:10.3109/1040841X.2013.841639.

22. Chiang, W.-C.; Nilsson, M.; Jensen, P.Ø.; Høiby, N.; Nielsen, T.E.; Givskov, M.; Tolker-Nielsen, T. Extracellular DNA Shields against Aminoglycosides in *Pseudomonas aeruginosa* Biofilms. *Antimicrob. Agents Chemother.* **2013**, *57*, 2352–2361, doi:10.1128/AAC.00001-13.

23. Huang, J.X.; Blaskovich, M.A.T.; Pelingon, R.; Ramu, S.; Kavanagh, A.; Elliott, A.G.; Butler, M.S.; Montgomery, A.B.; Cooper, M.A. Mucin Binding Reduces Colistin Antimicrobial Activity. *Antimicrob. Agents Chemother.* **2015**, *59*, 5925–5931, doi:10.1128/AAC.00808-15.

24. Landry, R.M.; An, D.; Hupp, J.T.; Singh, P.K.; Parsek, M.R. Mucin–*Pseudomonas aeruginosa* Interactions Promote Biofilm Formation and Antibiotic Resistance. *Mol. Microbiol.* **2006**, *59*, 142–151, doi:10.1111/j.1365-2958.2005.04941.x.

25. Puja, H.; Bolard, A.; Noguès, A.; Plésiat, P.; Jeannot, K. The Efflux Pump MexXY/OprM Contributes to the Tolerance and Acquired Resistance of *Pseudomonas aeruginosa* to Colistin. *Antimicrob. Agents Chemother.* **2020**, *64*, e02033-19, doi:10.1128/AAC.02033-19.

26. Dinesh, S.D. Artificial Sputum Medium. *Protoc Exch* **2010**.

27. Sønderholm, M.; Kragh, K.N.; Koren, K.; Jakobsen, T.H.; Darch, S.E.; Alhede, M.; Jensen, P.Ø.; Whiteley, M.; Kühl, M.; Bjarnsholt, T. *Pseudomonas aeruginosa* Aggregate Formation in an Alginate Bead Model System Exhibits In Vivo-Like Characteristics. *Appl. Environ. Microbiol.* **2017**, *83*, doi:10.1128/AEM.00113-17.

28. Bos, A.C.; Passé, K.M.; Mouton, J.W.; Janssens, H.M.; Tiddens, H.A.W.M. The Fate of Inhaled Antibiotics after Deposition in Cystic Fibrosis: How to Get Drug to the Bug? *J. Cyst. Fibros.* **2017**, *16*, 13–23, doi:10.1016/j.jcf.2016.10.001.

29. Cao, B.; Christophersen, L.; Kolpen, M.; Jensen, P.Ø.; Sneppen, K.; Høiby, N.; Moser, C.; Sams, T. Diffusion Retardation by Binding of Tobramycin in an Alginate Biofilm Model. *PLOS ONE* **2016**, *11*, e0153616, doi:10.1371/journal.pone.0153616.

30. Gordon, C.A.; Hodges, N.A.; Marriott, C. Antibiotic Interaction and Diffusion through Alginate and Exopolysaccharide of Cystic Fibrosis-Derived *Pseudomonas aeruginosa*. *J. Antimicrob. Chemother.* **1988**, *22*, 667–674, doi:10.1093/jac/22.5.667.

31. Martin, C.; Low, W.; Gupta, A.; Amin, M.; Radecka, I.; Britland, S.; Raj, P.; Kenward, K. Strategies for Antimicrobial Drug Delivery to Biofilm. *Curr. Pharm. Des.* **2014**, *21*, 43–66, doi:10.2174/1381612820666140905123529.

32. Bjarnsholt, T.; Jensen, P.Ø.; Fiandaca, M.J.; Pedersen, J.; Hansen, C.R.; Andersen, C.B.; Pressler, T.; Givskov, M.; Høiby, N. *Pseudomonas aeruginosa* Biofilms in the Respiratory Tract of Cystic Fibrosis Patients. *Pediatr. Pulmonol.* **2009**, *44*, 547–558, doi:10.1002/ppul.21011.

33. da Silva, L.V.R.F.; Ferreira, F. de A.; Reis, F.J.C.; de Britto, M.C.A.; Levy, C.E.; Clark, O.; Ribeiro, J.D. *Pseudomonas aeruginosa* Infection in Patients with Cystic Fibrosis: Scientific Evidence Regarding Clinical Impact, Diagnosis, and Treatment. *J. Bras. Pneumol. Publicaçã̃o Of. Soc. Bras. Pneumol. E Tisilogia* **2013**, *39*, 495–512, doi:10.1590/S1806-37132013000400015.

34. Bagge, N.; Schuster, M.; Hentzer, M.; Ciofu, O.; Givskov, M.; Greenberg, E.P.; Høiby, N. *Pseudomonas aeruginosa* Biofilms Exposed to Imipenem Exhibit Changes in Global Gene Expression and β-Lactamase and Alginate Production. *Antimicrob. Agents Chemother.* **2004**, *48*, 1175–1187.

35. Ciofu, O.; Tolker-Nielsen, T. Tolerance and Resistance of *Pseudomonas aeruginosa* Biofilms to Antimicrobial Agents—How *P. aeruginosa* Can Escape Antibiotics. *Front. Microbiol.* **2019**, *10*, doi:10.3389/fmicb.2019.00913.

36. Deschamps, E.; Schaumann, A.; Schmitz-Afonso, I.; Afonso, C.; Dé, E.; Loutelier-Bourhis, C.; Alexandre, S. Membrane Phospholipid Composition of *Pseudomonas aeruginosa* Grown in a Cystic Fibrosis Mucus-Mimicking Medium. *Biochim. Biophys. Acta BBA - Biomembr.* **2021**, *1863*, 183482, doi:10.1016/j.bbamem.2020.183482.

37. Cianciulli Sesso, A.; Lilić, B.; Amman, F.; Wolfinger, M.T.; Sonnleitner, E.; Bläsi, U. Gene Expression Profiling of *Pseudomonas aeruginosa* Upon Exposure to Colistin and Tobramycin. *Front. Microbiol.* **2021**, *12*.

38. Yu, Z.; Zhu, Y.; Fu, J.; Qiu, J.; Yin, J. Enhanced NADH Metabolism Involves Colistin-Induced Killing of Bacillus Subtilis and Paenibacillus Polymyxa. *Molecules* **2019**, *24*, 387, doi:10.3390/molecules24030387.

Supplementary materials

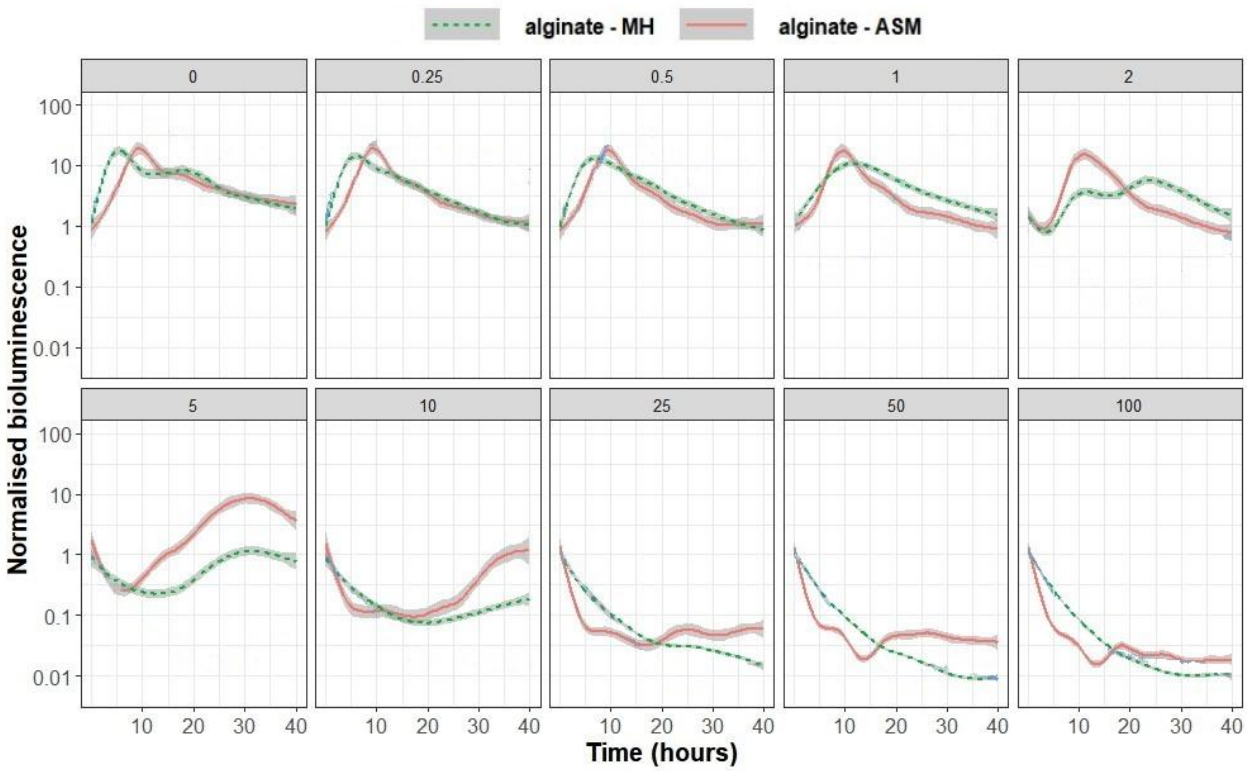

Figure S1: Bioluminescence kinetics of *P. aeruginosa* trapped in 60 µm-diameter **alginate beads dispersed in MHB or ASM exposed to different TOB concentrations expressed as a multiple of the MIC (MIC_{TOB} = 0.5 mg/L)**